

1 **Modeling of Facade Leaching in Urban Catchments**

S. Coutu,¹ D. Del Giudice,^{1, 2, 3} L. Rossi,¹ and D. A. Barry¹

¹Laboratoire de technologie écologique,
Institut d'ingénierie de l'environnement,
Faculté de l'environnement naturel,
architectural et construit (ENAC), Station
2, École Polytechnique Fédérale de
Lausanne (EPFL), 1015 Lausanne,
Switzerland.

²Now at: Eawag, Swiss Federal Institute
for Aquatic Science and Technology,
Ueberlandstrasse 133, 8600 Duebendorf,
Switzerland.

³Also at: Swiss Federal Institute of
Technology Zürich (ETHZ), 8093 Zürich,
Switzerland.

Abstract.

Building facades are protected from microbial attack by incorporation of biocides within them. Flow over facades leaches these biocides and transports them to the urban environment. A parsimonious water quantity/quality model applicable for engineered urban watersheds was developed to compute biocide release from facades and their transport at the urban basin scale. The model couples two lumped sub-models applicable at the basin scale, and a local model of biocide leaching at the facade scale. For the facade leaching, an existing model applicable at the individual wall scale was utilized. The two lumped models describe urban hydrodynamics and leachate transport. The integrated model allows prediction of biocide concentrations in urban rivers. It was applied to a 15-km² urban hydrosystem in western Switzerland, the Vuachère river basin, to study three facade biocides (terbutryn, carbendazim, diuron). The water quality simulated by the model matched well most of the pollutographs at the outlet of the Vuachère watershed. The model was then used to estimate possible ecotoxicological impacts of facade leachates. To this end, exceedance probabilities and cumulative pollutant loads from the catchment were estimated. Results showed that the considered biocides rarely exceeded the relevant Predicted No-Effect Concentrations for the riverine system. Despite the heterogeneities and complexity of (engineered) urban catchments, the model application demonstrated that a computationally “light” model can be employed to simulate the hydrograph and pollu-

24 tograph response within them. It thus allows catchment-scale assessment of
25 the potential ecotoxicological impact of biocides on receiving waters.

1. Introduction

26 Biocides are active, ecotoxic substances used for material protection via reduction of
27 microbially induced deterioration [Burkhardt *et al.*, 2007, 2009]. Urban-derived biocides
28 have received less attention than agricultural pesticides, for example, mainly due to their
29 underestimation in terms of both usage and potential for impairing water quality [Wittmer
30 *et al.*, 2011a]. Recently, biocide discharge rates in waters of a semi-urban catchment were
31 found to be up to an order of magnitude higher than agricultural pesticide discharges.
32 Furthermore, they can be bioaccumulative and persistent (i.e., low degradation rates) in
33 the environment, which make them a source of considerable concern [Burkhardt *et al.*,
34 2011].

35 A major source of biocides in urban environments is facade leaching of paints under wet-
36 weather conditions [Wittmer and Burkhardt, 2009; Burkhardt *et al.*, 2011]. Compounds
37 applied as biocides have been detected in combined sewer overflows (CSOs), in effluents of
38 urban wastewater treatment plants (WWTPs), and stormwater drains [Burkhardt *et al.*,
39 2007; Wittmer *et al.*, 2010]. Via these pathways, biocides can enter natural water bodies
40 such as lakes and rivers situated downstream of urban areas. Experimental investiga-
41 tions on biocide release from building envelopes have been reported at the facade [e.g.,
42 Schoknecht *et al.*, 2009; Burkhardt *et al.*, 2011] and sub-catchment scales [e.g., Burkhardt
43 *et al.*, 2007]. Recently, Wittmer *et al.* [2011b] and Coutu *et al.* [2012a] reported modeling
44 studies that considered wash-off of biocides from treated facades. However, no mathe-
45 matical model that predicts the transport and fate of biocides in urban catchments once
46 released from facades has been presented.

47 Environmental risk assessment of facade biocides requires modeling of their release from
48 facades to their eventual possible arrival in receiving waters. Such a model can be built by
49 coupling of appropriate hydrodynamic and water quality models. The need for integrated
50 models that are capable of simulating pollutographs of diffuse or point-source pollution
51 is recognized as an important challenge in urban hydrology [*Zoppou, 2001; Freni et al.,*
52 *2011*], and recent literature has pointed to the need for such models [*Delleur, 2003; Elliott*
53 *and Trowsdale, 2007; Jacobson, 2011*]. For risk assessment, features necessary in such a
54 model include the ability to capture urban hydrodynamics and associated water quality
55 signals on short time scales [*Elliott and Trowsdale, 2007*].

56 Our aim is to present a model for prediction of facade-sourced biocide in receiving
57 waters, which will be capable of forecasting the temporal variability of dissolved biocides
58 at the urban basin scale. An existing lumped-parameter hydrological model that has
59 proven its efficiency to replicate flow dynamics in engineered watersheds is adopted [*Coutu*
60 *et al., 2012b*]. This sub-model is coupled to biocide generation (facade-level, upscaled to
61 catchment scale) and transport modules of commensurate complexity, in order to create
62 an integrated model able to predict the facade-biocide response of an urban watershed.
63 The model is then field-validated and subsequently applied to predict risk of biocides in
64 natural waters.

2. Modeling Approach

2.1. Urban Hydrology

65 In order to assess the pollutant response of a hydrosystem, it is first necessary to re-
66 produce correctly its hydrologic response. A lumped model is used to predict discharge
67 dynamics at the outlet of the urban river basin. As noted by *Samaniego et al. [2010]*, such

68 parsimonious models are computationally efficient compared with fully distributed sim-
69 ulators. At the same time, these tools offer the advantage of providing an interpretable
70 representation of the hydrological behavior of the catchment [*Fenicia et al.*, 2006] and
71 have been successfully tested for diffuse sources of pollution in rural environments (e.g.,
72 *Rinaldo et al.* [2006] or *Basu et al.* [2010]). Here, the drainage basin is modeled as a set of
73 three reservoirs, each one characterized by a state variable representing the water storage
74 in the compartment (Figure 1). The two meteorological forcings to the hydrosystem are
75 precipitation, j , and air temperature, \mathcal{T} , both of which are assumed to be uniform over
76 the watershed.

77 **Figure 1 near here**

78 Both overland and subsurface water flow are considered. The surface compartment,
79 responsible for surface runoff, is modeled as a fast-reacting (transient) storage character-
80 ized by a water volume of S_s [cp., *Fenicia et al.*, 2007]. The subsurface flow is modeled
81 using two reservoirs: the vadose (or root) zone region and the groundwater region with,
82 respectively, storages of S_u and S_g [*Botter et al.*, 2010]. The root-zone and groundwater
83 reservoirs are considered to be extended over the total surface of the catchment, whereas
84 the surface compartment occupies only the pervious fraction (Figure 1). The groundwater
85 reservoir controls baseflow to the river. The total hydrologic response of the watershed,
86 Q_{tot} , is computed by combining linearly the (transient) outflow produced by the reservoirs.
87 Details of the hydrological framework are given by *Coutu et al.* [2012b].

2.2. Pollutant Generation on Facades and Basin-scale Transport

88 **Figure 2 near here**

89 In this section, a water quality model that can be coupled with the lumped catchment
90 flow model shown in Figure 1 is presented. The modeling approach groups biocide pro-
91 cesses into (i) generation (input), (ii) removal and (iii) transport.

92

93 **2.2.1. Biocide Generation**

94 Biocide is released from paints and renders that protect facades from biologically in-
95 duced deterioration. Transport of biocide from leached facades is considered here. Re-
96 cently, *Coutu et al.* [2012a] presented a single-facade leaching model that takes into account
97 facade length. On a given individual facade, their two-compartment model simulates the
98 leaching process as the transfer of biocide from one compartment (the wall) to another
99 (surface flow on the facade). In the wall matrix, the biocide migrates to the wall surface
100 following a diffusion-limited process, which is represented as an exponential decay. Once
101 on the surface of the facade, the biocide is available for leaching. Leaching to rainwater
102 runoff and exchange between the runoff and the wall surface is modeled with detachment-
103 deposition rates. Leached biocide is advected in the rainwater to the bottom of the facade.
104 Diffusion within the runoff volume is not considered. Figure 3 illustrates the dynamics of
105 biocides at facade scale.

106 **Figure 3 near here**

107 The model takes into account building height, a feature that allows simulation of leach-
108 ing of a collection of buildings using cadastral data. By this approach, upscaled (basin
109 scale) estimates of facade leaching based on cadastral data are possible. This upscaling

110 relies on the assumption that leaching of a given facade is independent of any other, such
111 that the response of the distribution of facade lengths (and other relevant cadastral data)
112 can be summed linearly over the distribution. In practice, we simplified the distribution
113 to its mean, i.e., the upscaled facade leaching estimates were based on mean amount of
114 biocide per unit area, total facade surface, mean facade height, and mean age of facade
115 coatings. In other words, the basin-scale response is based on the average facade in the
116 urban area considered, an approach that gives very similar results to those using the dis-
117 tribution of facades [Coutu *et al.*, 2012a]. Then, the facade-leaching model provides the
118 temporal distribution of the biocide as a function of rainfall. The dynamics of biocide
119 mass at the facade bottom are given by m_{fac} , and reflects catchment-averaged weather
120 conditions (rainfall intensity and wind direction).

121 **2.2.2. Removal Processes**

122 Contaminated water leaving the average facade can reach surface flow, or enter the soil.
123 To simplify matters as much as possible, we assume that biocide in water entering the
124 soil is sorbed or otherwise removed, whereas biocides in the overland flow do not undergo
125 any alterations. We expand on the basis for this approach in the following.

126 Biocides leached from facades can undergo a variety of processes, such as sorption,
127 degradation, etc., depending on the circumstances. The separation of the water entering
128 the soil after contact with the facade and that reaching the overland is included in the
129 parameter k_{isd} . Specifically, k_{isd}^{-1} of the leached biocide reaches the surface water flow,
130 with the rest entering the soil. In urban conditions, buildings are usually surrounded by
131 trenches or gardens designed to enhance infiltration of water flowing from facades, thus
132 the vast majority of the biocide will enter the soil rather than surface runoff, in which

133 case $k_{isd} \gg 1$. Biocides reaching the soil are considered to be completely immobilized or
 134 degraded since (i) the three studied pollutants show a high affinity to soil, as confirmed
 135 by relatively high soil-water partition coefficients (see Table 1), and (ii) once in the soil,
 136 biocides can undergo uptake processes, microbial degradation, hydrolysis or other degra-
 137 dation phenomena [Appelo and Postma, 2005]. Our simplified approach is consistent with
 138 recent work of Burkhardt *et al.* [2011]. They found that, during dry conditions, baseline
 139 biocide concentrations were below detection limits in urban receiving streams, whereas
 140 high concentrations were detected in stormwater runoff. Biocide that does not enter the
 141 soil is transported over impervious surfaces with runoff, where it is considered as com-
 142 pletely mixed with stormwater. This runoff water can either reach the sewer network
 143 (and hence the WWTP) or the river system (for an urban area equipped with a partially
 144 separated sewer system), as is calculated in the hydrological sub-model. In our model
 145 application, we consider biocide data for a river, not a WWTP.

The solute mass flux emitted by building facades, \dot{m}_{fac} , is thus reduced as follows:

$$\dot{m}_{in}(t) = \frac{\dot{m}_{fac}(t)}{k_{isd}} p_{hyb}, \quad (1)$$

146 where k_{isd} is the scaling factor accounting for the partitioning of runoff from facades, and
 147 p_{hyb} is the proportion of stormwater flow diverted to the river (i.e., $1 - p_{hyb}$ is diverted to
 148 the WWTP). In fact, when modeling a river basin including an urban area equipped with
 149 a partially separated sewer system (hybrid, *hyb*), a fraction of stormwater, and therefore
 150 of biocide, is diverted to the WWTP through the pipe system. The mass flux from facades
 151 that enters the overland flow is denoted by \dot{m}_{in} . Note that $k_{isd} \geq 1$ and $0 \leq p_{hyb} \leq 1$.

152 2.2.3. Biocide Transport

The residual mass flow rate available for transport, \dot{m}_{in} , enters the surface hydrologic reservoir, which is considered to be a completely mixed linear reactor with two dynamic variables, biocide mass, m , and water volume, S_s . The rate of change of pollutant mass in this one-compartment model is given by:

$$\dot{m} = \dot{m}_{in} - \dot{m}_{out} = \dot{m}_{in} - \frac{Q_{sup}}{S_s}m. \quad (2)$$

153 The biocide flux out of the surface reservoir is given by \dot{m}_{out} in equation 2. This equation
 154 and all other differential equations of the model were solved using a first-order Euler
 155 scheme. Although this scheme is often considered as poorly stable [Beers, 2006], it was
 156 found to be efficient in this context. Furthermore, other numerical methods (not presented
 157 here) were tested with no changes observed in the results.

158 The biocide concentration of at the outlet of the watershed, C_{out} , is given by:

$$C_{out}(t) = \frac{\dot{m}_{out}(t)}{Q_{tot}(t)}, \quad (3)$$

159 where $Q_{tot} = Q_{sup} + Q_{sub}$ is the total hydrological response of the catchment.

160 The procedure leading to the construction of the integrated water quantity and quality
 161 model is summarized in Figure 2. The biocide mass flux from the upscaled facade-leaching
 162 sub-model is transferred to the transport sub-model. This biocide flux from the basin's fa-
 163 cades is reduced by a certain factor (p_{hyb}/k_{isd}) to account for different removal phenomena,
 164 as described previously. In summary, the contaminant compartment receives the residual
 165 biocide flux, which is mixed with surface water to create a bi-variable compartment-model.
 166 The biocide discharged is further diluted by the stream flow.

167 **2.2.4. Calibration Procedure**

168 A two-component metric was adopted to calibrate the water quality model. Note that
169 k_{isd} is the only calibrated parameter of the biocide transport model. The quality of the
170 prediction was estimated using the Nash-Sutcliffe (NS, optimal value of one) and the
171 Normal-Bias (NB, optimal value of 0) coefficients. The optimization used [Hingray *et al.*,
172 2009]:

$$\text{Min}\{(1 - NS) + |NB|\}. \quad (4)$$

173 This multicriteria calibration procedure is recommended for better comprehension of the
174 model performance [Hingray *et al.*, 2009]. Note that the hydrological model was calibrated
175 separately in another study [Coutu *et al.*, 2012b]. Separation of the hydrological and water
176 quality calibrations is warranted in order to obtain satisfactory concentration simulations
177 without impacting on the water discharge predictions [Kirchner, 2006].

3. Case Study

3.1. Site Description

178 **Table 1 near here**

179 The model was applied to a meso- γ scale system [Orlanski, 1975], the Vuachère river
180 basin, located in the eastern part of the city of Lausanne, Switzerland (Figure 4). The total
181 area of the catchment is 15 km², of which approximately 34% is covered by impervious
182 surfaces. According to data reported by Jordan [2010], about 60% of runoff generated
183 on these surfaces contributes to the river discharge, while the rest flows into the sewer
184 system. This value of 0.6, the “separation proportion”, corresponds to the loss factor p_{hyb} .

185 Through a GIS analysis (<http://www.swisstopo.admin.ch/>, site last accessed on 28
186 August 2012) of cadastral data, the total surface area and mean height of the catchment's
187 buildings were estimated as, respectively, 8.8×10^6 m² and 17 m. According to *Coutu*
188 *et al.* [2012a], windows and doors lead to a reduction of about one third of the facade
189 area. Data for Switzerland on facade biocide treatment in 2007 [*Wittmer et al.*, 2011a]
190 were taken as representative for the Vuachère river basin: 60% of facades have biocide
191 treatment. We examined three major biocides, which were considered to have been applied
192 according to their market share: carbendazim 40%, diuron 30%, and terbutryn 30%.

193 To estimate the actual masonry surface which undergoes leaching during rain, the preva-
194 lent wind direction must be considered. Indeed, wind velocity along with building char-
195 acteristics influence the amount of rain coming into contact with facades and thus affect
196 the amount of biocides leached. Facades exposed to the prevalent wind direction undergo
197 greater leaching than protected facades. On average about 75% of the basin's facades
198 [*Blocken and Carmeliet*, 2004; *Abuku et al.*, 2009; *Coutu et al.*, 2012a] are protected in
199 any given rain event.

200 Taking these factors into account, the facade surface area exposed to leaching in the
201 Vuachère basin was estimated as 8.8×10^5 m².

202 **Figure 4 near here**

3.2. Experimental Data at the Vuachère River Outlet

203 Water quantity and quality data were collected at the outlet of the Vuachère basin.
204 Discharge dynamics were calculated using continuously recorded water stages ([http://](http://echo.epfl.ch/)
205 echo.epfl.ch/, site last accessed on 28 August 2012).

206 Biocide concentration measurements were obtained through a sampling campaign. As
207 described by *Ort et al.* [2010], concentration dynamics should be determined on the basis
208 of appropriate sampling intervals, in order to increase the likelihood of capturing concen-
209 tration pulses. Although sampling intervals depend on the characteristics of the catchment
210 and chemicals under investigation, high frequency sampling is recommended (> 1 sample
211 h^{-1}).

212 Transport of facade biocides is controlled by rain events [e.g., *Wittmer et al.*, 2011a].
213 Thus, concentration spikes will occur with storm hydrographs. Based on these considera-
214 tions, an automatic sampler was programmed to draw a series of aliquots after a certain
215 water level was exceeded in the Vuachère river. In total, biocide concentrations were
216 measured for four storm events of modest intensity in spring 2011. Storm events were
217 respectively 6 h, 1 h, 40 min and 4 h long, with a total rainfall of 8.5, 2.5, 3.5 and 7 mm,
218 respectively.

4. Results and Discussion

4.1. Hydrographs and Pollutographs

219 Figure 5 shows the comparison between measured and simulated discharges during the
220 sampling period. This hydrograph was discussed by *Coutu et al.* [2012b], where the
221 hydrological model (§2.1) was presented and validated. We do not repeat that discussion
222 here, but simply show the hydrograph as it is essential to prediction of the pollutograph.

223 **Figure 5 near here**

224 Since the hydrological simulator reproduces satisfactorily the observed discharge time
225 series, the biocide portion of the model is examined. For each substance, the reduction

226 factor, k_{isd} , was calibrated. The results of the model adjustment, in terms of water quality
227 predictions, are presented in Figures 6 and 8.

228 **Figure 6 near here**

229 We see in Figure 6 that the response time of the pollutograph is a few hours whereas
230 half-lives of the considered substances are in the range of several days (Table 1), which
231 is consistent with our assumption that no degradation occurs during the runoff process.
232 The data indicate that the biocide concentration increases rapidly after the rain starts,
233 behavior that is reproduced by the model. However, due to the fact that the program-
234 ming of the sampling device was recorded to take samples after a certain water level was
235 exceeded, the decay of biocide concentrations was only partially recorded.

236 Figure 7 shows that biocide concentrations follow roughly linearly the impulsive rise of
237 the river flow at the beginning of the rain event. The response is fast for flow and biocides,
238 as additional water responsible for flow rise is generated principally by impervious surfaces
239 in the steep, urbanized Lausanne basin. This initial episodic concentration behavior comes
240 from the dynamics of the source model (see Figure 3 and [Coutu *et al.*, 2012a]). During dry
241 weather, biocides accumulate on facade surfaces at rainfall start and are readily removed
242 by rainfall. When the flow rate starts to decrease, concentrations remain high so long
243 as the surface runoff contribution dominates inflow to the river. As indicated above, in
244 our model surface runoff controls biocide concentrations because biocides in water that
245 infiltrates the soil are sorbed or degraded. Subsurface flow contributes to the stream
246 hydrograph on longer time scales than the flashy surface runoff. In consequence, biocide

247 concentrations decrease during the hydrograph recession, as contribution of non-polluted
248 infiltrated water increases.

249 **Figure 7 near here**

250 The measured and computed pollutographs at the outlet of the hydrosystem exhibit
251 close agreement. The model allows prediction of biocide dynamics at a high temporal
252 resolution, which is controlled by the flow model input data. Previous studies have shown
253 the complexity of matching data from a high resolution sampling campaign and model
254 results [*Massoudieh et al.*, 2008]. Also, because of the complexity of organizing automatic
255 high-frequency sampling campaigns, solute transport models are often calibrated using
256 averaged concentrations, with averages taken over an hour or more [e.g., *Matsui et al.*,
257 2006; *Riml and Wörman*, 2011], rather than the high frequency dynamics of biocide
258 transport that are captured here.

259 **Figure 8 near here**

260 In our model, the scaling parameter k_{isd} describes the partitioning of facade-emitted
261 biocide at the catchment scale. However, for such a simplified approach we do not expect
262 that k_{isd} correlates with the sorption coefficient K_d , as k_{isd} represents partitioning of
263 water from facades as well as all biogeochemical degradation processes as well as spatial
264 variability that the biocide undergoes during its transfer from the facade to the river
265 outlet. In addition, there is considerable uncertainty in the mass of the three different
266 substances on facades, which in our case was based on a Swiss study (see §3.1). It is
267 likely that the distribution of these substances on the considered basin varies, albeit in a

268 manner that has not been determined, which could also underpin the lack of correlation
269 observed between K_d and k_{isd} .

270 The calibrated hydrologic-transport model was employed to study cumulative biocide
271 loads released from facades and reaching Lake Geneva via the Vuachère River over 1 y
272 (May 2010-April 2011). Results are plotted in Figure 9 for cumulative loads computed at
273 the facade bottom and the river outlet. Storms occurring after dry periods produce more
274 intense biocide release than those taking place after wet weather since, as already noted,
275 biocides accumulate on facade surfaces during these periods [*Burkhardt et al.*, 2011; *Coutu*
276 *et al.*, 2012a].

277 Only a small portion of biocides emitted by facades exit the basin. Figure 9 shows
278 that around 0.35% of the leached biocide mass reaches the outlet, which translates into
279 an annual load to Lake Geneva of approximately 25 g of each biocide. This figure must
280 be considered with caution due to the uncertainty of the integrated modeling approach,
281 principally in the amount of biocide available on facade surface [*Burkhardt et al.*, 2012;
282 *Coutu et al.*, 2012a]. In addition, the proposed methodology did not consider transport
283 of biocides via particulate matter. Even so, based on our results it is possible to estimate
284 roughly the amount of biocides reaching receiving waters in Switzerland, assuming that
285 the Vuachère basin can be considered as representative. Large amounts of biocides are
286 used annually in urban areas of Switzerland [*Wittmer and Burkhardt*, 2009]. *Coutu et al.*
287 [2012a] estimated that approximately 30% of applied facade coatings are leached annually,
288 and so are available for transfer from facade bottoms to receiving waters. *Wittmer and*
289 *Burkhardt* [2009] and *Burkhardt et al.* [2011] estimated that, conservatively speaking,
290 about 100 tons of biocides are used annually for facade protection in Switzerland. From

291 these values, we estimate that in Switzerland about 100 kg of biocides are transferred
292 to receiving waters each year, and that hundreds of kilograms infiltrate into soils. This
293 estimate might be a lower bound, as it does not consider biocides that are routed to
294 WWTPs.

295 **Figure 9 near here**

4.2. Risk Analysis

296 To analyze the environmental risk of computed biocide loads, a statistical analysis of
297 stream concentrations was performed. In Figure 10, the Predicted No-Effect Concentra-
298 tions (PNECs) of the considered biocides [*Burkhardt et al.*, 2009] are plotted together with
299 the concentration duration curves, representing the probability that the biocide's concen-
300 tration at the catchment exit is exceeded during the year. The figure illustrates that the
301 calibrated model computes concentrations that are mostly lower than the environmental
302 PNEC. Diuron is the only exception, although it has only a low probability of exceeding
303 its critical value. Again, results of the risk analysis should be taken with caution due to
304 the abovementioned uncertainties.

305 **Figure 10 near here**

306 The calibrated model occasionally underpredicted measured concentrations, sometimes
307 by a factor of two. In consequence, a safety factor of two may be applied to the modelling
308 results when performing risk assessment. In terms of risk frequency, this would corre-
309 spond to using half the PNEC values presented in Figure 10. To apply this safety factor
310 of two would lead to new exceedance probabilities: 9% for diuron and 5% for carben-

311 dazim to exceed PNEC/2. The exceedance probability for terbutryn remains zero. Note
312 that exceedance probabilities were computed by including dry weather and wet weather
313 periods. If rainy periods are considered only, probability for a substance to exceed PNEC
314 is obviously increased substantially, since it is during these periods that most biocide is
315 transported.

4.3. Limitations

316 As discussed above, during rain, the dynamics of concentration peaks are reproduced
317 satisfactorily by the integrated model. During some storm events, however, the model
318 predictions and the measured data show differences, up to a factor of about two, as al-
319 ready stated. This is possibly because we assumed that facades are the only source of
320 biocides to streams, although biocides can be applied for other uses (e.g., agricultural)
321 [*Wittmer and Burkhardt, 2009*]. The absence of secondary sources could be responsible for
322 the underestimation of the pollutograph of each solute at the catchment outlet. Also, our
323 model treats rainfall as uniform over the catchment, whereas of course it varies spatially,
324 which would interact with the spatial distribution of applied biocides in the catchment.
325 A localized study would be necessary to investigate this issue. On the other hand, our
326 model has the virtue of properly matching the pollutograph not only for one event and
327 substance but for most of the events of all chemicals. Given the high uncertainty inher-
328 ent to urban environment, especially for substances at nanogram level, we consider the
329 modeling performance achieved as satisfactory.

330 It is interesting to observe that the facade model implicitly supposes that the temporal
331 response of all biocides to rainfall events is the same. The model then propagates this
332 behavior through the entire system. In other words, the coupled model assumes that all

333 biocides have the same dynamics but different initial quantities and reduction factors. This
334 behavior is a significant prediction that can be tested in studies of different catchments,
335 with different transport characteristics.

5. Conclusions

336 Biocides leach from building facades and are transported to receiving waters. To ana-
337 lyze their transport at the urban basin scale, a ‘top-down’ hydrologic approach has been
338 adopted [e.g., *Sivapalan*, 2006; *Savenije*, 2009; *Basu et al.*, 2010], leading to the creation
339 of a parsimonious, multiprocess biocide transport model. The model includes upscaling
340 and coupling of a facade-scale leaching model with basin-scale hydrologic and biocide
341 transport sub-models. The majority of biocides leached from facades are removed before
342 reaching receiving waters. The model includes simple scaling factors that lump these
343 removal processes into a single, basin-scale value.

344 The modeling framework proposed was applied to simulate the response (viz., hydro-
345 graphs and pollutographs) of a steep, partly urbanized Swiss river basin. The integrated
346 model was tested using monitoring data collected at the outlet of the catchment. The hy-
347 drodynamics of the Vuachère river basin were reproduced with reasonable accuracy by the
348 quasi-linear simulator developed. The simulator also showed a good facility in matching
349 measured pollutographs, with concentrations predicted to within a factor of about two,
350 although generally the model provided underpredictions. Since the model traces biocides
351 from building facades in the catchment, this agreement between model predictions and
352 data (both in timing and in magnitude) suggests that facades are, indeed, main source of
353 the considered biocides found in the Vuachère.

354 Encouraged by the satisfactory model validation, we proceeded to estimate the annual
355 biocide load from the Vuachère basin facades to Lake Geneva. The analysis revealed that
356 concentrations were most of the time below PNEC values, and that the total biocide load
357 to the lake was of the order of a few tens of grams per year. One proviso to this estimate
358 is that our field sampling and modeling did not account for biocides transported with
359 particles in overland flow.

360 The model makes use of highly simplified descriptions of the transport process from
361 facade to basin outlet. It is, perhaps, surprising that it performs with the demonstrated
362 accuracy. Its success corroborates the applicability of the well-mixed modeling approx-
363 imation to basin-scale transport phenomena, where the size of the injection areas (viz.
364 urban surfaces) is much larger than that of heterogeneous features [*Rinaldo et al.*, 2006].
365 In this vein, it shows that structural heterogeneity of soil and land uses, characterizing
366 semi-urbanized zones, does not prevent a conceptually simple, parsimonious hydrological
367 modeling approach from being applied in a realistic setting. However, for each biocide
368 considered, the predicted pollutograph relies on fitting of a single parameter, k_{isd} . That
369 is, calibration of this model parameter is mandatory before predictions can be made.

370 The flexibility of this methodology permits the future inclusion of other nonpoint sources
371 of aquatic contamination. Furthermore, because the model is computationally undemand-
372 ing, it allows the possibility of simulating pollutographs for large numbers of urban systems
373 for the purpose of environmental risk assessment and design of protection strategies for
374 downstream ecosystems. On the other hand, the model predictions are based on a large
375 reduction in mass from facades, due to the retention of biocides by soil. This reduction
376 was obtained by calibration, and could not be correlated in any obvious way with the

377 biocide sorption characteristics. Further investigation on whether the reduction factor,
378 k_{isd} , could be predicted independently is thus warranted.

379 **Acknowledgments.** The authors thank Htet Kyi Wynn, who was responsible for lab-
380 oratory analysis of the water samples, Emilie Grand, who participated in field measure-
381 ments and installation of sampling devices, and Bernard Sperandio, who provided the
382 river flow data. The City of Lausanne is also acknowledged for providing information on
383 the Vuachère river catchment. We would also like to thank the reviewers for the care they
384 took in reviewing this manuscript. Their contribution significantly helped in making the
385 manuscript more comprehensive.

Appendix: Definition of the different symbols used in this study.

386 **Table 2 near here**

Notes

- 387 1. [Burkhardt et al., 2009]
2. [Prichard et al., 2005]
3. <http://www.cdpr.ca.gov/docs/emon/pubs/fatememo/diuron.pdf>, site last accessed on 02.04.2012
4. http://www.epa.gov/espp/litstatus/effects/diuron_efed_chapter.pdf, site last accessed on 02.04.2012
5. [Dores et al., 2009]
6. [Avidov et al., 1985]
7. <http://extoxnet.orst.edu/pips/terbutry.htm>, site last accessed on 02.04.2012
8. [Wu et al., 1974]
9. [Barriuso et al., 1992]
10. http://www.sea.eawag.ch/inhalt/sites/stoffe/pdf/Biozide_e.pdf, site last accessed on 02.04.2012
11. [Berglof et al., 2002]

References

- 388 Abuku, M., H. Janssen, J. Poesen, and S. Roels (2009), Impact, absorption and evap-
389 oration of raindrops on building facades, *Building and Environment*, 44(1), 113–124,
390 doi:10.1016/j.buildenv.2008.02.001.
- 391 Appelo, C., and D. Postma (2005), *Geochemistry, groundwater and pollution*, Taylor &
392 Francis Group, Leiden, The Netherlands.
- 393 Avidov, E., N. Aharonson, J. Katan, B. Rubin, and O. Yarden (1985), Persistence of
394 terbutryn and atrazine in soil as affected by soil disinfestation and fungicides, *Weed*
395 *Science*, 33, 457–461.

- 396 Barriuso, E., C. Feller, R. Calvet, and C. Cerri (1992), Sorption of atrazine, terbutryn
397 and 2,4-D herbicides in two Brazilian Oxisols, *Geoderma*, *53*(1-2), 155–167, doi:10.1016/
398 0016-7061(92)90028-6.
- 399 Basu, N., P. S. C. Rao, H. E. Winzeler, S. Kumar, P. Owens, and V. Merwade (2010),
400 Parsimonious modeling of hydrologic responses in engineered watersheds: Structural
401 heterogeneity versus functional homogeneity, *Water Resources Research*, *46*, W04501,
402 doi:10.1029/2009WR007803.
- 403 Beers, K. (2006), *Numerical methods for chemical engineering: Applications in Matlab*,
404 Cambridge University Press, Cambridge, U.K., ISBN: 9780521859714.
- 405 Berglof, T., T. V. Dung, H. Kylin, and I. Nilsson (2002), Carbendazim sorption-desorption
406 in Vietnamese soils, *Chemosphere*, *48*(3), 267–273, doi:10.1016/S0045-6535(02)00096-6.
- 407 Blocken, B., and J. Carmeliet (2004), A review of wind-driven rain research in building
408 science, *Journal of Wind Engineering and Industrial Aerodynamics*, *92*(13), 1079–1130,
409 doi:10.1016/j.jweia.2004.06.003.
- 410 Botter, G., E. Bertuzzo, and A. Rinaldo (2010), Transport in the hydrologic response:
411 Travel time distributions, soil moisture dynamics, and the old water paradox, *Water*
412 *Resources Research*, *46*, W03514, doi:10.1029/2009WR008371.
- 413 Burkhardt, M., T. Kupper, S. Hean, R. Haag, P. Schmid, M. Kohler, and M. Boller (2007),
414 Biocides used in building materials and their leaching behavior to sewer systems, *Water*
415 *Science and Technology*, *56*(12), 63–67, doi:10.2166/wst.2007.807.
- 416 Burkhardt, M., M. Junghans, S. Zuleeg, M. Boller, U. Schoknecht, X. Lamani, K. Bester,
417 R. Vonbank, and H. Simmler (2009), Biozide in gebaudefassaden-okotoxikologische ef-
418 fekte, auswaschung und belastungsabschätzung für gewässer, *Umweltwissenschaften und*

- 419 *Schadstoff-Forschung*, 21, 36–47.
- 420 Burkhardt, M., S. Zuleeg, R. Vonbank, P. Schmid, S. Hean, X. Lamani, K. Bester, and
421 M. Boller (2011), Leaching of additives from construction materials to urban storm
422 water runoff, *Water Science and Technology*, 63(9), 1974–1982, doi:10.2166/wst.2011.
423 128.
- 424 Burkhardt, M., S. Zuleeg, R. Vonbank, K. Bester, J. Carmeliet, M. Boller, and T. Wangler
425 (2012), Leaching of biocides from facades under natural weather conditions, *Environ-
426 mental Science and Technology*, 46(10), 5497–5503, doi:10.1021/es2040009.
- 427 Coutu, S., L. Rossi, C. Rota, and D. A. Barry (2012a), Modelling city-scale facade leaching
428 of biocide by rainfall, *Water Research*, 46, 3525–3534, doi:10.1016/j.watres.2012.03.064.
- 429 Coutu, S., D. D. Giudice, L. Rossi, and D. A. Barry (2012b), Parsimonious hydrological
430 modeling of urban sewer and river catchments, *Journal of Hydrology*, (*in press*), doi:
431 10.1016/j.jhydrol.2012.07.039.
- 432 Delleur, J. (2003), The evolution of urban hydrology: Past, present, and future, *Journal
433 of Hydraulic Engineering-ASCE*, 129, 563–573, doi:10.1061/(ASCE).
- 434 Dores, E., C. Spadotto, O. Weber, L. Carbo, A. Vecchiato, and A. Pinto (2009), Environ-
435 mental behaviour of metolachlor and diuron in a tropical soil in the central region of
436 Brazil, *Water, Air, & Soil Pollution*, 197(1), 175–183, doi:10.1007/s11270-008-9801-1.
- 437 Elliott, A., and S. Trowsdale (2007), A review of models for low impact urban stormwater
438 drainage, *Environmental Modelling & Software*, 22(3), 394–405, doi:10.1016/j.envsoft.
439 2005.12.005.
- 440 Fenicia, F., D. Solomatine, H. Savenije, and L. Hoffmann (2006), An approach to multi-
441 criteria calibration of hydrologic models and their mixtures, in *Geophysical Research*

- 442 *Abstracts*, vol. 8, p. 06834, doi:1607-7962/gra/EGU06-A-06834.
- 443 Fenicia, F., H. H. G. Savenije, P. Matgen, and L. Pfister (2007), A comparison of alter-
444 native multiobjective calibration strategies for hydrological modeling, *Water Resources*
445 *Research*, *43*, W03434, doi:10.1029/2006WR005098.
- 446 Freni, G., G. Mannina, and G. Viviani (2011), Assessment of the integrated urban water
447 quality model complexity through identifiability analysis, *Water Research*, *45*(1), 37–50,
448 doi:10.1016/j.watres.2010.08.004.
- 449 Hingray, B., C. Picouet, and A. Musy (2009), *Hydrologie 2: Une science pour l'ingénieur*,
450 Science et ingénierie de l'environnement, Presses Polytechniques et Universitaires Ro-
451 mandes, Lausanne, Switzerland.
- 452 Jacobson, C. R. (2011), Identification and quantification of the hydrological impacts of
453 imperviousness in urban catchments: A review, *Journal of Environmental Management*,
454 *92*(6), 1438–1448, doi:10.1016/j.jenvman.2011.01.018.
- 455 Jordan, F. (2010), Modélisation du réseau d'assainissement: Outil de diagnostic et de
456 planification en ville de Lausanne, *GWA. Gas, Wasser, Abwasser*, *90*(3), 199–208.
- 457 Kirchner, J. (2006), Getting the right answers for the right reasons: Linking measure-
458 ments, analyses, and models to advance the science of hydrology, *Water Resources*
459 *Research*, *42*, W03S04, doi:10.1029/2005WR004362.
- 460 Massoudieh, A., A. Abrishamchi, and M. Kayhanian (2008), Mathematical modeling of
461 first flush in highway storm runoff using genetic algorithm, *Science of the Total Envi-*
462 *ronment*, *398*(1-3), 107–121, doi:10.1016/j.scitotenv.2008.02.050,.
- 463 Matsui, Y., K. Narita, T. Inoue, and T. Matsushita (2006), Screening level analysis for
464 monitoring pesticide in river water using a hydrological diffuse pollution model with

- 465 limited input data, *Water Science & Technology*, 53(10), 173–181.
- 466 Orlanski, I. (1975), A rational subdivision of scales for atmospheric processes, *Bulletin of*
467 *the American Meteorological Society*, 56(5), 527–534.
- 468 Ort, C., M. G. Lawrence, J. Rieckermann, and A. Joss (2010), Sampling for pharmaceuti-
469 cals and personal care products (PPCPs) and illicit drugs in wastewater systems: Are
470 your conclusions valid? A critical review, *Environmental Science & Technology*, 44(16),
471 6024–6035, doi:10.1021/es100779n.
- 472 Prichard, T., J. Troiano, J. Marade, F. Guo, and M. Canevari (2005), Movement of
473 diuron and hexazinone in clay soil and infiltrated pond water, *Journal of Environmental*
474 *Quality*, 34, 2005–2017, doi:10.2134/jeq2004.0253.
- 475 Riml, J., and A. Wörman (2011), Response functions for in-stream solute transport in
476 river networks, *Water Resources Research*, 47, W06502, doi:10.1029/2010WR009412.
- 477 Rinaldo, A., G. Botter, E. Bertuzzo, A. Uccelli, T. Settin, and M. Marani (2006), Trans-
478 port at basin scales: 1. Theoretical framework, *Hydrology and Earth System Sciences*,
479 10, 19–29, doi:1607-7938/hess/2006-10-19.
- 480 Samaniego, L., R. Kumar, and S. Attinger (2010), Multiscale parameter regionalization of
481 a grid-based hydrologic model at the mesoscale, *Water Resources Research*, 46, W05523,
482 doi:10.1029/2008WR007327.
- 483 Savenije, G. (2009), HESS Opinions “The art of hydrology”, *Hydrology and Earth System*
484 *Sciences*, 13(2), 157–161.
- 485 Schoknecht, U., J. Gruycheva, H. Mathies, H. Bergmann, and M. Burkhardt (2009),
486 Leaching of biocides used in facade coatings under laboratory test conditions, *Environ-*
487 *mental Science & Technology*, 43(24), 9321–9328, doi:10.1021/es9019832.

- 488 Sivapalan, M. (2006), *Pattern, Process and Function: Elements of a Unified Theory of*
489 *Hydrology at the Catchment Scale, Encyclopedia of Hydrological Sciences.*, John Wiley
490 & Sons, Ltd, Chichester, U. K., doi:10.1002/0470848944.hsa012.
- 491 Wittmer, I. K., and M. Burkhardt (2009), Dynamics of biocide and pesticide input, *Eawag*
492 *News, 67ff/*, 8–11.
- 493 Wittmer, I. K., H. P. Bader, R. Scheidegger, H. Singer, A. Luck, I. Hanke, C. Carlsson,
494 and C. Stamm (2010), Significance of urban and agricultural land use for biocide and
495 pesticide dynamics in surface waters, *Water Research, 44*(9), 2850–2862, doi:10.1016/
496 j.watres.2010.01.030.
- 497 Wittmer, I. K., R. Scheidegger, H. P. Bader, H. Singer, and C. Stamm (2011a), Loss
498 rates of urban biocides can exceed those of agricultural pesticides, *Science of the Total*
499 *Environment, 409*(5), 920–932, doi:10.1016/j.scitotenv.2010.11.031.
- 500 Wittmer, I. K., R. Scheidegger, C. Stamm, W. Gujer, and H. Bader (2011b), Modelling
501 biocide leaching from facades, *Water Research, 45*, 3453–3460, doi:10.1016/j.watres.
502 2011.04.003.
- 503 Wu, C., P. Santelmann, and J. Davidson (1974), Influence of soil temperature and moisture
504 on terbutryn activity and persistence, *Weed Science*, pp. 571–574.
- 505 Zoppou, C. (2001), Review of urban storm water models, *Environmental Modelling &*
506 *Software, 16*(3), 195–231, doi:10.1016/S1364-8152(00)00084-0.

Table 1. Characteristics of the most common biocides found in surface waters [*Wittmer and Burkhardt, 2009; Wittmer et al., 2010, 2011a*].

Biocides	Function	Usages	Main driving factors	Half-life (d)	K_d ($l\text{ kg}^{-1}$)	PNEC ¹ ($ng\text{ l}^{-1}$)
Diuron	Herbicide, algicide	Facades, preservatives, pesticide (fruit, asparagus), etc.	Urban rain-driven	Soils: 90 ² , water: > 43 ^{3,4}	3.1-14.7 ⁵	20
Terbutryn	Herbicide, algicide	Bathrooms, facades, etc.	Urban rain-driven, urban continuous	Soils: 14-28 ^{6,7} , water: 180-240 ⁸	1.5-18.2 ^{8,9}	34
Carbendazim	Fungicide	Bathrooms, facades, pesticide (fruit, vegetables), etc.	Urban rain-driven, household	Soils: 8-32 ¹⁰ , water: stable ¹¹	8.1-35 ¹¹	34

Table 2. Definitions of the different symbols used in this study.

Symbol	Definition	Dimension
A_i	impervious area of the catchment	$[L^2]$
A_p	pervious area of the catchment	$[L^2]$
ET	evapotranspiration	$[L T^{-1}]$
j	precipitation rate	$[L T^{-1}]$
m_{fac}	mass of pollutant at facade bottom	$[M]$
Q_{sub}	discharge streamflow of S_g	$[L^3 T^{-1}]$
Q_{sup}	discharge streamflow of S_s	$[L^3 T^{-1}]$
S_g	subsurface reservoir	$[L^3]$
S_s	impervious/fast-reacting reservoir	$[L^3]$
S_u	vadose zone reservoir	$[L^3]$
\mathcal{T}	temperature	$[\Theta]$

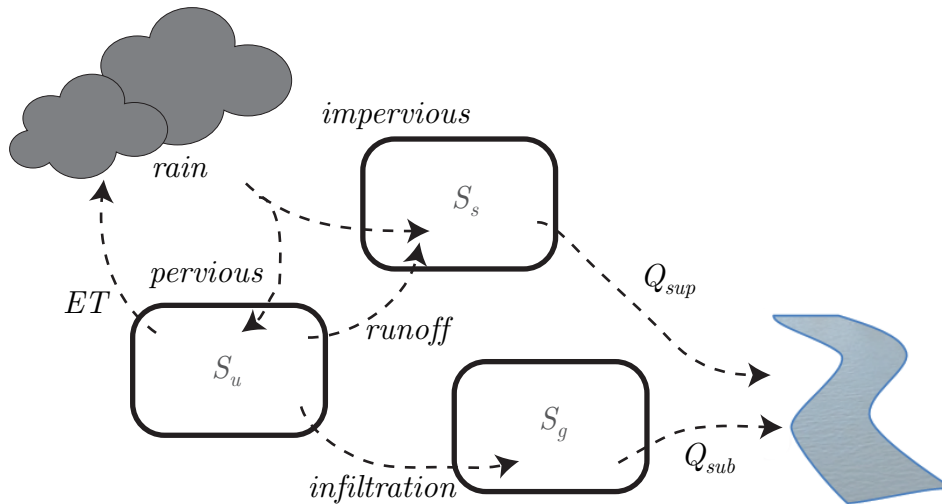


Figure 1. Model of urban watershed flow [Coutu *et al.*, 2012b]. Rainwater (j) lands on pervious (S_u) or impervious (S_s) surfaces in proportion to the exposure of each surface type. When the rainfall flux exceeds that maximum soil infiltration capacity, runoff occurs from the pervious to the impervious area. Water from the impervious area is discharged rapidly (Q_{sup}) to the river through the drainage system. Water in the vadose zone (S_u) flows to a subsurface reservoir (S_g) that discharges slowly (Q_{sub}) to the river. Model equations defining these fluxes are presented in Coutu *et al.* [2012b].

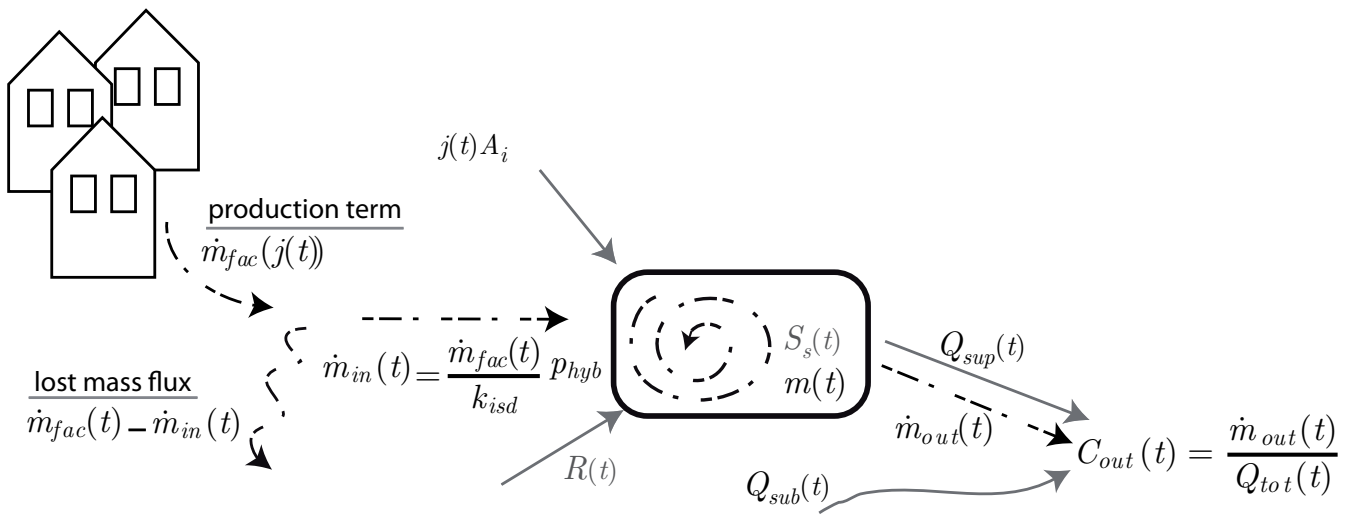


Figure 2. Schematic representation of the basin-scale biocide transport model. Biocides leach from facades at a rate \dot{m}_{fac} , based on upscaling the model of *Coutu et al.* [2012a]. Some biocide is diverted out of the river catchment through the combined sewer system (a fraction $1 - p_{hyb}$) and some is lost due infiltration/sorption/degradation (a fraction $(1 - k_{isd})/k_{isd}$, see equation 1). The remaining fraction (\dot{m}_{out}) mixes in the surface reservoir with rainwater (jA_i) and is flushed to the river (\dot{m}_{out}), where it is mixed in the total flow (Q_{tot}). Solid arrows show water transport and dashed arrows illustrate biocide pathways.

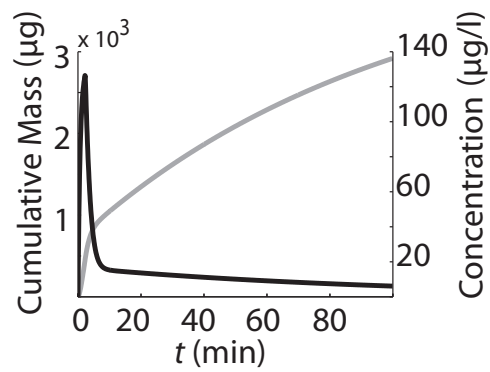


Figure 3. Dynamics of simulated load (grey) and concentration (black) of a typical biocide at the bottom of a 2 m high facade during a constant rain event. The presented curve can be affected by facade height and paint age. More details on the modeling can be found in *Coutu et al.* [2012a].

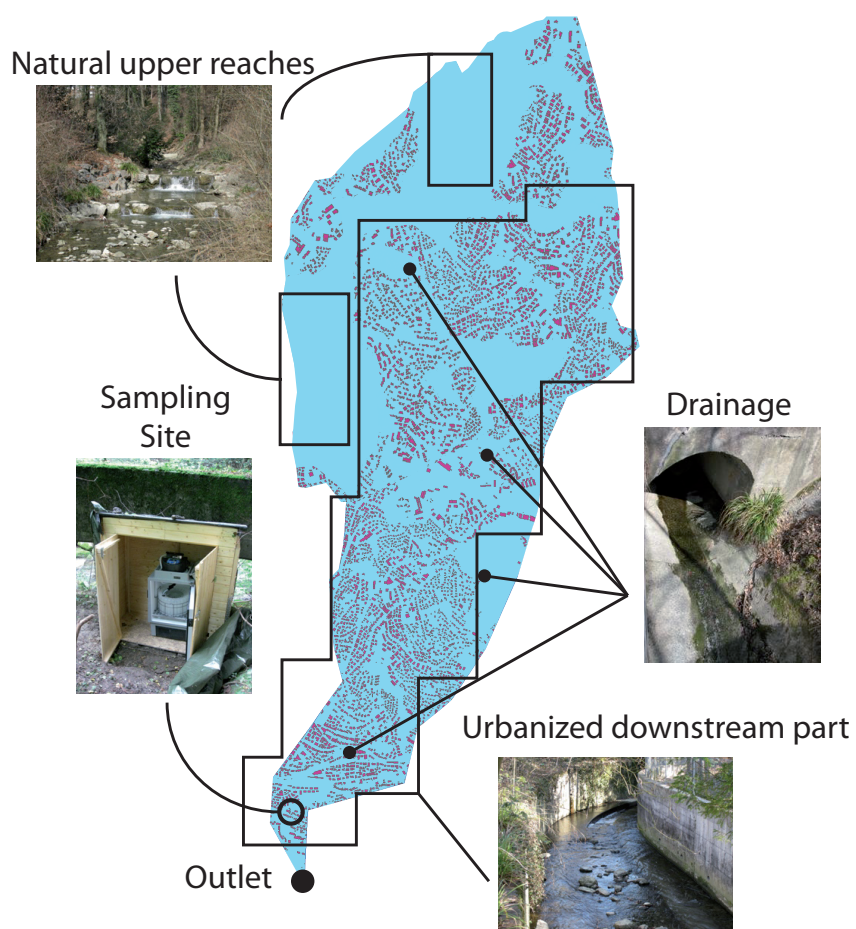


Figure 4. Overview of the Vuachère river basin. Buildings are represented by pink polygons, while the colored area is the drainage basin. The drainage system takes rainfall runoff (and biocides) to the river. The sampling site is located close to river outlet.

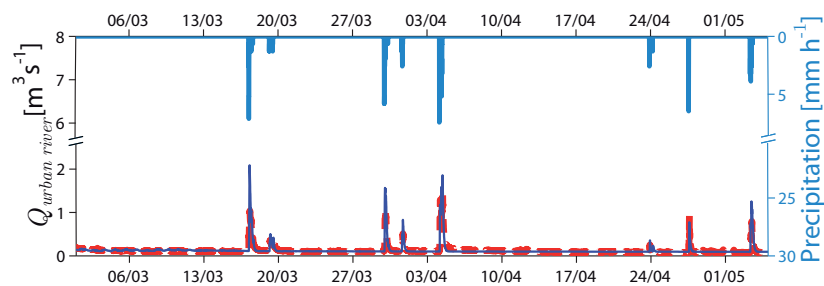


Figure 5. Predicted (line) and measured (dots) flow rate at the outlet of Vuachère river basin. Precipitation is shown in blue on the right vertical axis [Coutu *et al.*, 2012b].

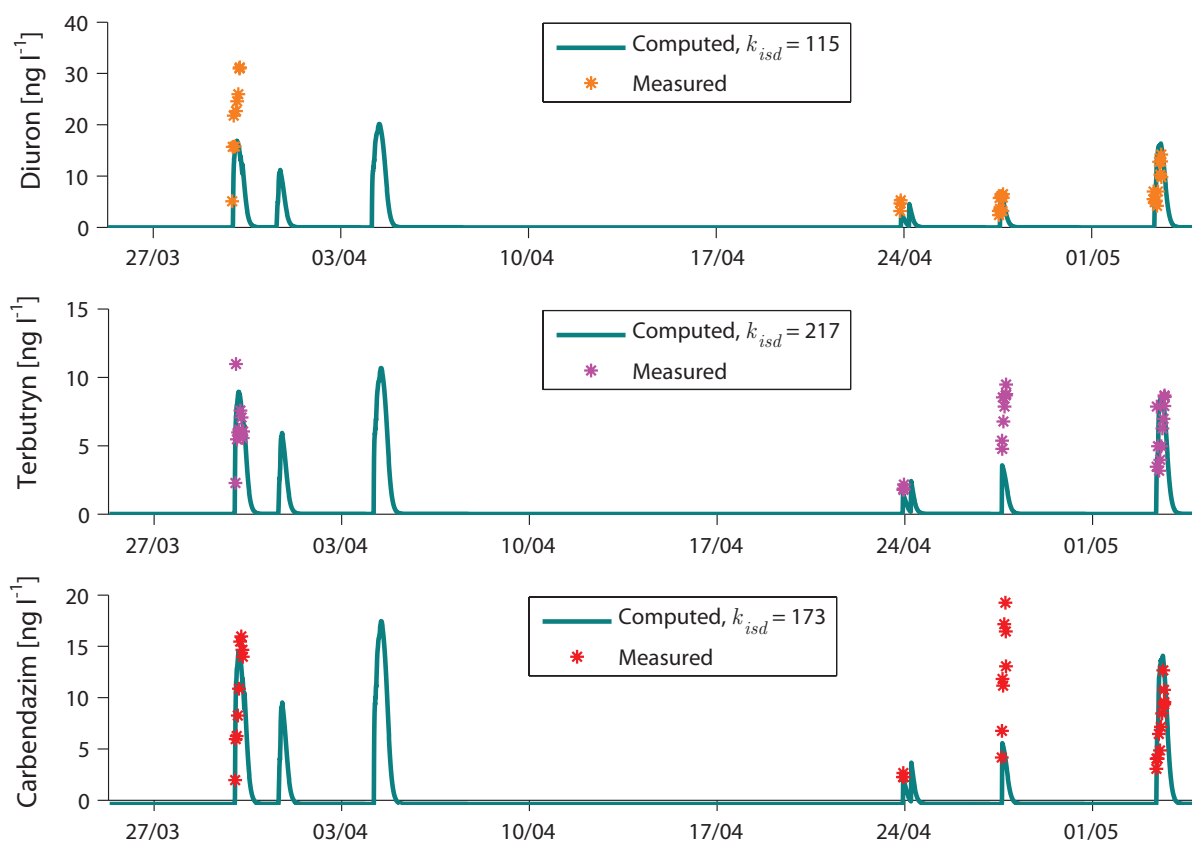


Figure 6. Comparison between observed and simulated pollutographs for the Vuachère hydrosystem. Three substances were investigated: diuron, terbutryn, carbendazim. Two rainfall events were not sampled (03/31 and 04/04).

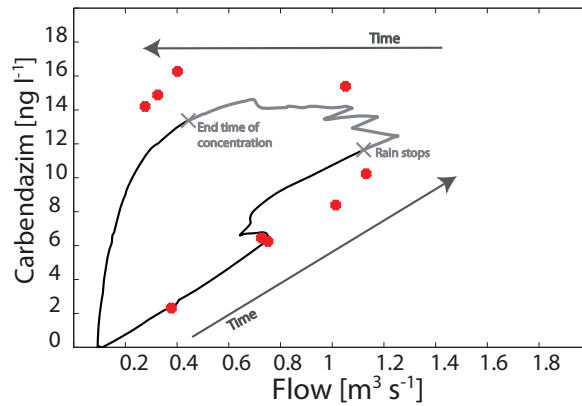


Figure 7. Carbendazim concentration against flow for the first peak in concentration observed (see Figure 6, 29/03). Data are shown as points and predictions as the solid line. The concentration increases roughly linearly with flow during the flow buildup phase. When the flow rate decreases, the concentration varies little for a certain period before decaying exponentially to zero. As mentioned in the text, concentration measurements were not collected during the decay period. The cessation of rainfall is indicated with a cross. The time of concentration of the studied basin (~ 2 h) is illustrated with the grey line. After this time period, the contribution of infiltrated water (Q_{sub}) starts to dominate the global hydrograph instead of surface runoff (Q_{sup}). According to our modelling approach, the infiltrated water is free of biocide.

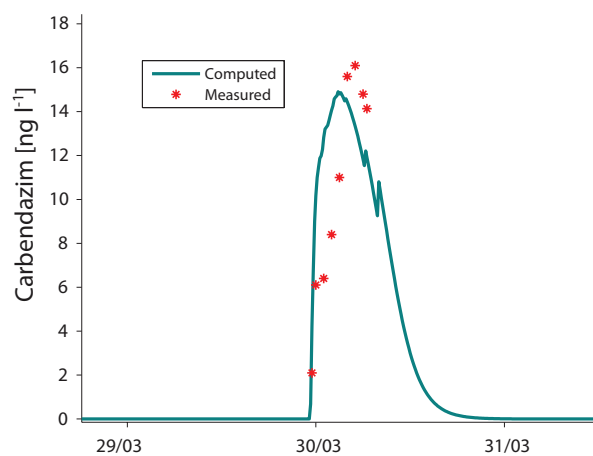


Figure 8. Enlarged view of the first concentration peak (observed and modeled, 29/03 on Figure 6) for carbendazim.

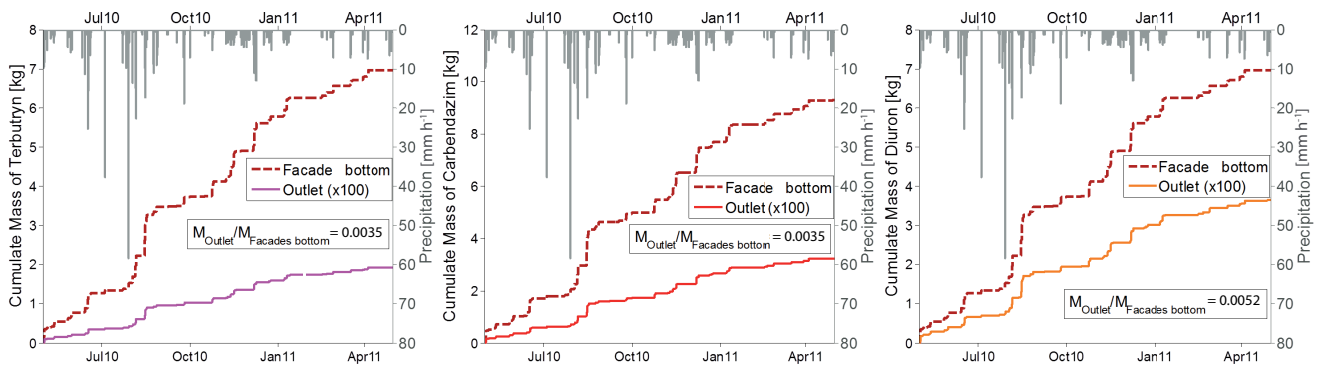


Figure 9. Cumulative input and output biocide masses for the Vuachère hydrosystem, released by precipitation events. The accumulated load at the outlet of the watershed is multiplied by 100 for the sake of visualization. The ratio of the two annual loads is also shown.

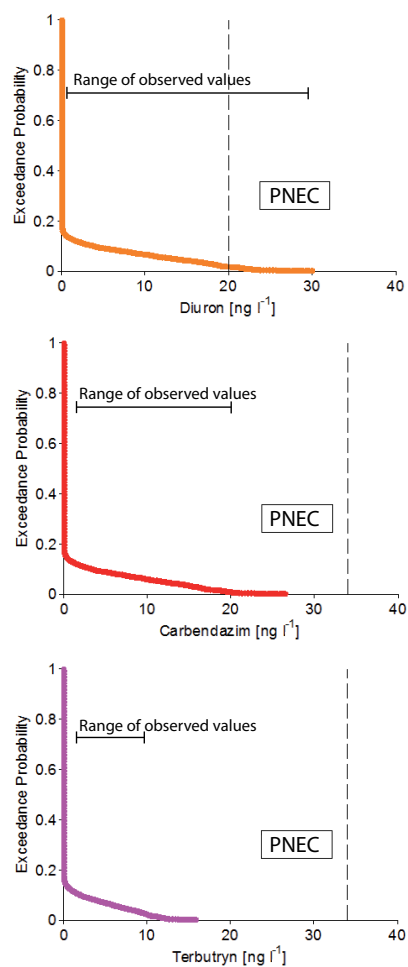


Figure 10. Complementary cumulative distribution function of computed concentrations over 1 y at the outlet of the Vuachère watershed. Critical values for each pollutant are also shown (dashes). The PNEC is exceeded (4% probability) only for Diuron.